

# Angular 21 cm Power Spectrum of a Scaling Distribution of Cosmic String Wakes

Oscar F. Hernández<sup>2,1\*</sup>, Yi Wang<sup>1†</sup>, Robert Brandenberger<sup>1‡</sup> and José Fong<sup>3,1§</sup>

*1) Department of Physics, McGill University, Montréal, QC, H3A 2T8, Canada*

*2) Marianopolis College, 4873 Westmount Ave., Westmount, QC, H3Y 1X9, Canada and*

*3) Ecole Normale Supérieure, Lyon, France*

Cosmic string wakes lead to a large signal in 21 cm redshift maps at redshifts larger than that corresponding to reionization. Here, we compute the angular power spectrum of 21 cm radiation as predicted by a scaling distribution of cosmic strings whose wakes have undergone shock heating.

PACS numbers: 98.80.Cq

## I. INTRODUCTION

A new observational window to probe the structure of the universe is opening up: 21 cm redshift surveys. Such surveys offer the prospect of mapping out the distribution of neutral hydrogen in the universe, and thus will be able to probe the distribution of matter in the “dark ages”, before star formation sets in (see [1] for an extensive review). Regions in space which have an overdensity of baryons will lead to excess emission or absorption signals in 21 cm redshift maps.

In a previous paper [2] we considered the signal of a single cosmic string in a 21 cm redshift map. Cosmic strings moving through space produce nonlinear matter overdensities in their wakes - even at redshifts larger than that of reionization. We pointed out that cosmic strings which are relevant to cosmological structure formation will leave a large imprint in 21 cm redshift surveys, in particular at redshifts larger than that corresponding to reionization, a redshift range where the “noise” from reionization processes is not present. As will be briefly reviewed below, we found that a single cosmic string gives a characteristic signal in 21 cm redshift maps: a wedge which is thin in redshift direction and extended in both angular directions (see Figure 1). The planar extent of the wedge is set by the length of the string at the time it is formed, and the wedge thickness depends on the string tension. The angular extent of the signal from a string wake produced at the time of recombination is of the order of  $1^\circ$ , and the mean thickness  $\delta z$  of the wedge in redshift direction (which depends on the tension of the string) is about  $\delta z/z \sim 10^{-4}$  if the string tension  $\mu$  is given by  $G\mu = 10^{-7}$  ( $G$  being Newton’s gravitational constant) and the string is moving with a velocity close to the speed of light. The brightness temperature of the string signal depends both on the redshift of string formation and that of 21 cm emission, but only very mildly on the string tension. The 21 cm brightness temperature of a wake at a redshift  $z_e + 1 = 20$  can be of the order of  $-15$  mK for strings formed during matter radiation equality with  $G\mu = 10^{-7}$ . Based on this large signal we expect that it will be much easier to see the signals of strings - if they are present - in 21 cm maps than in other cosmological windows of observation.

There has recently been renewed interest in the cosmological effects of cosmic strings (see e.g. [3–7] for reviews on cosmic strings and their effects in cosmology). It has been realized that many particle physics models beyond the Standard Model of particle physics give rise to cosmic strings. Such strings arise, for example, at the end of inflation in many supergravity models [8]. Similarly, cosmic strings are a generic remnant of many models of brane inflation [9].

Furthermore, if strings exist, there will not be just one. In models which lead to cosmic strings, a network of strings will inevitably form in a phase transition in the early universe. Causality arguments [10] then imply that these strings will persist at all times up to the present time. Both analytical arguments [3–5] and numerical simulations [11] tell us that the network of cosmic strings will take on a “scaling solution” in which the average quantities describing the network are invariant in time if measured in Hubble length  $H^{-1}(t)$ , where  $H$  is the expansion rate of space.

In this paper we will compute the angular power spectrum at fixed redshift produced by the distribution of cosmic strings emitting 21 cm radiation. Specifically, we are interested in the shape and overall amplitude of the signal. The paper is organized as follows: We begin in Section II with a brief review of cosmic string cosmology and observables of cosmic string wakes in 21 cm experiments. In Section III, we review the cosmic string toy model of [12] which we use, and construct the cosmic string wake profile and number statistics. In Section IV, we calculate the 21 cm power

---

\* oscarh@physics.mcgill.ca

† wangyi@physics.mcgill.ca

‡ rhb@physics.mcgill.ca

§ jose.fong@ens-lyon.fr

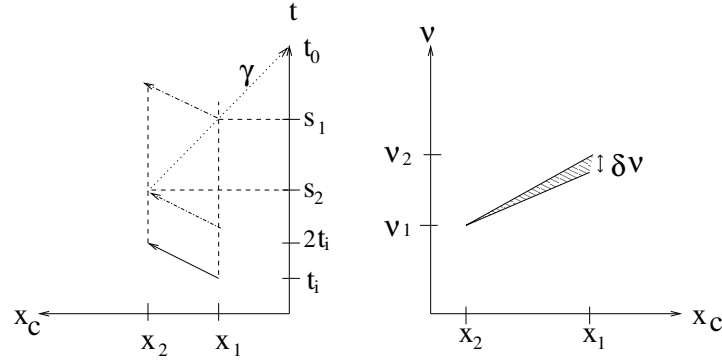


FIG. 1: Geometry of the 21 cm signal of a cosmic string wake. The left panel is a sketch of the geometry of the wake in space-time - vertical axis denoting time, the horizontal axis denoting one direction of space. The string segment producing the wake is born at time  $t_i$  and travels in the direction of the arrow, ending at the position  $x_2$  at the time  $2t_i$ . The past light cone of the observer at the time  $t_0$  intersects the tip of the wake at the time  $s_2$ , the back of the wake at time  $s_1$ . These times are in general different. Hence, the 21 cm radiation from different parts of the wake is observed at different red-shifts. The resulting angle-redshift signal of the string wake shown in the left panel is illustrated in the right panel, where the horizontal axis is the same spatial coordinate as in the left panel, but the vertical axis is the redshift of the 21 cm radiation signal. The wedge in 21 cm has vanishing thickness at the tip of the wedge, and thickness given by  $\delta v$  at the back side.

spectrum for these cosmic string wakes. Section IV contains the main result of the paper. Readers who are familiar with cosmic string wakes or 21 cm observations can skip Section II or Section III and jump directly to Section IV. In Section V we present our conclusions and put our work in context.

## II. COSMOLOGY OF COSMIC STRINGS AND THEIR WAKE'S BRIGHTNESS TEMPERATURE

Cosmic strings are lines<sup>1</sup> in space with trapped energy. It is the gravitational effects of this energy which leads to the role which the strings play in the formation of cosmological structure, as first pointed out in [13]. As relativistic objects they have tension equal to the mass per unit length and velocity  $v_s$  of the order  $c$ . Their relativistic nature is also responsible for the characteristic string signatures in cosmological observations - the fact that space perpendicular to a long straight string is not flat, but conical with deficit angle  $\alpha = 8\pi G\mu$  [14]. This deficit angle leads to gravitational lensing of microwave radiation about the string which in turn leads to a line discontinuity in the temperature on the CMB [15]. These line discontinuities can be searched for [16] using edge detection algorithms such as the Canny algorithm [17]. Maps with good angular resolution such as those that are being produced by the South Pole Telescope (SPT) [18] and Atacama Cosmology Telescope (ACT) [19] are ideally suited to search for cosmic strings.

A long straight cosmic string segment moving through space will lead to a wedge-shaped overdense region in its wake, a so-called "cosmic string wake" [20]. To understand what a wake is let us look at the physics from the point of view of an observer on the string. This observer will see matter streaming by on both sides. But since space is conical, the matter acquires a velocity  $\delta v$  given by

$$\delta v = 4\pi G\mu v_s \gamma(v_s) \quad (1)$$

towards the plane behind the string. This leads to the formation of a wedge of twice the background matter density behind the string. The wake, in turn, will grow in thickness by gravitational accretion, as studied e.g. in [21] using the Zel'dovich approximation. If a cosmic string is laid down at a redshift  $z_i$ , then the mean width of the wake (defined as the overdense region which has collapsed and undergone shock heating) at redshift  $z_e$  will be

$$w(t_e) = \frac{6\pi}{5} G\mu v_s \gamma(v_s) t_i \left[ \frac{(z_i + 1)}{(z_e + 1)} \right]^2. \quad (2)$$

The extra baryon density in the wake will lead to extra 21 cm absorption or emission. If the 21 cm radiation is

<sup>1</sup> These lines are in fact thin tubes with thickness given by a microphysical scale.

emitted from a wake at redshift  $z_e$  its brightness temperature is given by

$$\delta T_b(z_e) = [70 \text{ mK}] \frac{x_c}{1+x_c} \left(1 - \frac{T_\gamma}{T_K}\right) \frac{(1+z_e)^{1/2}}{2 \sin^2 \theta}. \quad (3)$$

Here  $T_\gamma$  is the CMB temperature,  $T_K$  is the wake gas kinetic temperature,  $\theta$  is the angle of the 21 cm ray with respect to the vertical to the wake, and  $x_c$  are the collision coefficients whose values can be obtained from the tables listed in [23]. Here and throughout we take the cosmological parameters to be  $H_0 = 73 \text{ km s}^{-1} \text{ Mpc}^{-1}$ ,  $\Omega_b = 0.0425$ ,  $\Omega_m = 0.26$ . We work with a matter dominated universe for  $z \leq 3000$  with the age of the universe  $t_0 = 4.3 \times 10^{17} \text{ s}$ .

Note the  $T_K$  and the  $\theta$  dependence in Eq. 3. The string tension and the string's speed affect the temperature  $T_K$  of the neutral hydrogen in the wake, while the string's direction of motion determines  $\theta$ . We simplify our calculations below by working with the brightness temperature of a string oriented so that  $2 \sin^2 \theta = 1$  and  $(v_s \gamma(v_s))^2 = 1/3$ . Thus the only string parameter that will determine the brightness temperature will be the string tension  $G\mu$ .

Whether the string signal is an emission or absorption signal (positive or negative brightness temperature, respectively) depends on the ratio between the wake temperature of neutral hydrogen and the temperature of the microwave photons. The former is larger at lower redshifts, the latter is larger at higher redshifts. At redshifts below  $z = 20$ , reionization effects become important so we consider 21 cm radiation emitted at  $z_e = 20$  from a string formed at the redshift  $z_i + 1 = 3000$  corresponding to the time  $t_{eq}$  of equal matter and radiation. We found [2] that the critical value of  $G\mu$  at which the transition from absorption to emission occurs is  $(G\mu)_6 \simeq 0.23$ , where  $(G\mu)_6$  is the string tension in units of  $10^{-6}$ .

### III. COSMIC STRING WAKE NETWORKS

#### A. Scaling solution

The scaling solution is characterized by a random walk-like network of “infinite” strings (length larger than the Hubble radius) with step length comparable to the Hubble radius, plus a distribution of string loops with radii  $R$  smaller than the Hubble radius. According to numerical simulations [11], the long strings dominate. For our study, we will make use of an analytical toy model for the distribution of strings first introduced in [12]: we divide the relevant time interval (in particular the time interval between  $t_{eq}$  and the present time  $t_0$ ) into Hubble time steps. At each step, space is divided up into boxes of Hubble size at the corresponding local times. In each time interval we lay down  $N_H$  straight cosmic string segments per Hubble volume. According to numerical simulations the value of  $N_H$  ranges from 1 to 10. Each string segment laid down at time  $t$  has a physical length at that time which is given by  $c_1 t$  (where  $c_1$  is a constant which is expected to be slightly smaller than 1, and whose value is expected to decrease as  $N_H$  increases) and depth given by  $v_s \gamma(v_s) t$ , where  $v_s$  is the velocity of the string in the plane perpendicular to its tangent vector, and  $\gamma(v_s)$  is the associated relativistic gamma factor. The value of  $v_s$  is expected to be of order one in units where the speed of light  $c$  is set to one.

The earliest Hubble time interval which we consider is at the time of equal matter and radiation, and the corresponding size of the spatial boxes at that time is  $t_1 = t(z_{eq})$ . The wakes produced by these strings are in fact both the most numerous (since a fixed comoving volume contains the largest number of wakes of that size) and the thickest (since the dark matter fluctuations have had the longest time to grow. The baryons are tightly coupled to radiation until the time  $t_{rec}$  of recombination but then fall into the potential wells created by the dark matter. String wakes laid down before  $t_{eq}$  will have a thickness which scales as  $(z(t_i) + 1)^{-1/2}$  since the dark matter perturbations cannot grow while the dark matter forms the subdominant component of matter.

Later time steps are centered at the values  $t_2 = 2t(z_{eq})$ ,  $\dots$ ,  $t_m = 2^{m-1}t(z_{eq})$  respectively. Thus the total number of these Hubble time steps is

$$M_{tot} = \text{Int} \left[ \log_2 \left( \frac{t_0 + t(z_{eq})}{t(z_{eq})} \right) \right] = \text{Int} \left\{ \log_2 \left[ 1 + (z_{eq} + 1)^{3/2} \right] \right\}, \quad (4)$$

where  $\text{Int}(x)$  is the integer part of  $x$ . Taking  $z_{eq} \simeq 3000$ , we have  $M_{tot} = 17$ . However, as we discuss later in Section III E, not all of these Hubble steps (at which the wakes are laid down) contribute to the 21 cm emission power spectrum.

At each Hubble step, the cosmic strings are taken to be “created” at the beginning of the Hubble step and “annihilated” at the end of the step. In reality, the string network is a complicated dynamical distribution. Since the strings are moving relativistically, intercommutation events of two strings are frequent. For a fixed string, it lasts typically about one Hubble time step until this string intersects another one. Such an intersection will lead to a coarsening of the network of long strings via the production of cosmic string loops and the consequent straightening of

the remaining long string network. Hence, we are modelling the distribution of the long string network in any Hubble time step as a collection of straight string segments which result from an initial intercommutation event at the time of “creation”, and undergo a next intercommutation at the time of “annihilation”. Since the intercommutation events are uncorrelated in space, it is a good approximation to consider the centers and directions of motion of the string segments to be randomly distributed, and uncorrelated from one time step to the next. Similarly, we expect a spread in the distribution of the velocities  $v_s$ .

The cosmic string wakes are produced by the motion of the strings through space. Once produced, the wakes will be approximately static in comoving coordinates, except for the growth in thickness due to gravitational accretion of the surrounding gas. We will consider the shape profile and number statistics of these wakes in the following subsections.

### B. Wake profile

A cosmic string segment laid down at time  $t_i$  will generate a wake whose physical dimensions at that time are

$$c_1 t_i \times t_i v_s \gamma_s \times 4\pi G \mu t_i v_s \gamma_s. \quad (5)$$

The dimensions  $c_1 t_i$  and  $t_i v_s \gamma_s$  span the two length dimensions of the wake and are independent of the string tension. They are both of the order of the instantaneous Hubble radius. The third dimension is the width of the wake, which is much smaller than the length because it is suppressed by the small parameter  $G\mu$ .

These three dimensions evolve with time. Firstly, the two length dimensions are comoving in space. Thus at a later time  $t_e$ , their physical size is

$$c_1 t_i \left( \frac{z_i + 1}{z_e + 1} \right) \times v_s \gamma_s t_i \left( \frac{z_i + 1}{z_e + 1} \right), \quad (6)$$

where  $z_i = z(t_i)$  and  $z_e = z(t_e)$ . For simplicity, in some of the later calculations, we shall use  $l(z_i, z_e)$  to denote the length of the wake at time  $t_e$  if the time of formation is  $t_i$ , ignoring the order one difference between these two dimensions.

The width of the wake will grow in time. According to linear perturbation theory it follows that the comoving width dimension grows linearly with the scale factor. We are interested in the width of the region which has collapsed and shock heated. The determination of this region can be done using the Zel'dovich approximation [22] and gives a result which is smaller than the naive linear perturbation theory result by approximately a factor of 4 [2]. The final result is given in (2).

### C. Wake Number Statistics: Method 1

For later use, we will calculate the number density of cosmic string wakes on a fixed redshift hypersurface in two ways, making use of two different approximations. Both calculations agree to within a factor of order one.

We shall use  $S^2$  to denote the hypersurface with fixed redshift  $z_e$  from which the 21 cm signals are emitted. The comoving radius  $r$  of this sphere can be calculated as

$$r(t_e) = \int_{t_e}^{t_0} \frac{dt}{a(t)} = \frac{3}{a_0} t_0^{2/3} (t_0^{1/3} - t_e^{1/3}), \quad (7)$$

where  $a_0$  is the value of the scale factor at the present time  $t_0$  and can be set to 1 without loss of generality.

At the time  $t_m$  when wakes in the  $m$ 'th Hubble time interval are laid down, the physical radius of the above  $S^2$  is

$$R_m = a(t_m) r(t_e) = 3 t_m^{2/3} (t_0^{1/3} - t_e^{1/3}). \quad (8)$$

Except at the final Hubble time steps close to the present time, this value of  $R_m$  is much greater than the Hubble scale  $1/H(t_m) = 3t_m/2$ , which is also the typical length of straight string segments. Thus, for our counting procedure, the string segments can be treated as point particles. Note that the length of the string wake is of the same order as the Hubble scale. This breaks the particle approximation which is made here. However, as we show in the next section, using a full string world sheet calculation, the simple and intuitive approximation made here leads to the correct result, up to a constant of order one.

The number of strings that pass through the  $S^2$  per unit area per unit time is

$$n_s \times v_s \times \cos \theta_s, \quad (9)$$

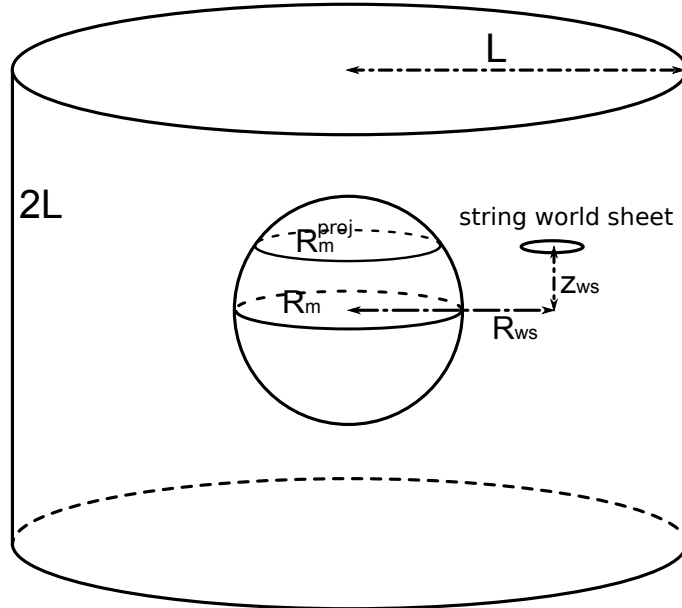


FIG. 2: Illustration of how the number of relevant wakes is computed in Section III D. Here the  $z_{sw}$  direction is chosen to be perpendicular to the string world sheet. And in the figure we have rotated the  $z$  direction to be the vertical direction only for the purpose of convenience.

where  $n_s$ ,  $v_s$ ,  $\theta_s$  denote the number density, averaged velocity and direction of motion of the cosmic strings, respectively. Thus, the number of strings that crosses the the  $S^2$  is

$$N_{S^2} = n_s \times v_s \times \cos \theta_s \times 4\pi R_m^2 \times 1/H(t_m) . \quad (10)$$

Since the cosmic string network achieves a scaling solution, it is more convenient to use number  $N_H$  of strings per Hubble volume instead of the number density of strings. Thus, we have

$$N_{S^2} = N_H \times v_s \times \cos \theta_s \times 4\pi R_m^2 \times H(t_m)^2 . \quad (11)$$

This  $N_{S^2}$  is also the number of wakes on the sphere where the 21 cm signal with redshift  $z_e$  were emitted.

The two dimensional number density of cosmic string wakes at the emission time  $t_e$  can be calculated as

$$n_{2D} = \frac{N_{S^2}}{4\pi a(t_e)^2 r^2} = \frac{4N_H v_s \cos \theta_s}{9t_m^2} \left( \frac{z_e + 1}{z_m + 1} \right)^2 . \quad (12)$$

For our examples below we have averaged the direction speed of motion such that  $\cos^2 \theta_s = 1/2$  and  $v_s = 1/2$ , and take  $N_H = 10$ ,  $t_m = 2.6 \times 10^{12}$  s for the first Hubble step ( $m = 1$ ) corresponding to  $z = 3000$ .

#### D. Wake Number Statistics: Method 2, a Worksheet Calculation

We calculate the probability that a string world sheet intersects the  $S^2$ . The string world sheet is created at  $t_m$ , and destroyed one Hubble time after that, with string length  $l_s$ . Note that the length scale  $l_s$  is of order  $t_m$ . Thus the current method should be more precise than the previous one.

For simplicity, we approximate the string world sheet as circular. The rectangular world sheet could also be calculable, but with the need of taking into account considerably more effects. We use  $r_{ws}$  to denote the radius of the circular world sheet. To best mimic a rectangular world sheet, we take the area of the world sheet to be unchanged while deforming its shape. Thus we have

$$\pi r_{ws}^2 = c_1 t_m \times t_m v_s \gamma_s , \quad r_{ws} = t_m \sqrt{c_1 v_s \gamma_s / \pi} . \quad (13)$$

Consider one single circular cosmic string world sheet, as shown in Figure 2. Without loss of generality, we consider the world sheet inside a cylindrical volume. The cylinder has volume  $2\pi L^3$ . Here we take  $L > R$ , where  $R$  is the

largest of the scales appearing in (13). The probability for the string world sheet (which is inside this cylinder) to intersect the  $S^2$  can be calculated as

$$\frac{1}{2\pi L^3} \int_{-R_m}^{R_m} dz_{\text{ws}} \int_0^L dR_{\text{ws}} \int_0^{2\pi} R_{\text{ws}} d\theta_{\text{ws}} \times \Theta(R_{\text{ws}} - R_m^{\text{proj}} + r_{\text{ws}}) \Theta(R_m^{\text{proj}} + r_{\text{ws}} - R_{\text{ws}}). \quad (14)$$

where  $\Theta(x)$  is the Heaviside step function, and  $R_m^{\text{proj}} \equiv \sqrt{R_m^2 - z_{\text{ws}}^2}$ . Keeping in mind that  $R_m \gg r_{\text{ws}}$ , the above integration yields

$$(\text{Probability}) \simeq \frac{\pi R_m^2 r_{\text{ws}}}{L^3}. \quad (15)$$

Thus, for  $N_{\text{ws}}$  world sheets, the number of intersections is  $N_{\text{ws}} \pi R_m^2 r_{\text{ws}} / L^3$ . The number of world sheets  $N_{\text{ws}}$  is related to the number density of world sheets (which equals to the number density of strings) by  $N_{\text{ws}} = 2\pi L^3 n_s$ . Thus, finally, we have

$$N_{S^2} = 2\pi^2 n_s R_m^2 r_{\text{ws}} = (4\pi n_s v_s R_m^2 H_m^{-1}) \left( \frac{\sqrt{\pi c_1 v_s \gamma_s}}{3v_s \cos \theta_s} \right). \quad (16)$$

When the factor  $\sqrt{\pi c_1 v_s \gamma_s} / (3v_s \cos \theta_s)$  is of order unity, this result is in agreement with the result (10).

### E. Cutting Off the Hubble Steps

For the calculations in [2] to hold the wake must undergo shock heating. This occurs when the kinetic temperature inside the wake is at least 2.5 times greater than the background gas temperature (the temperature of the matter particles outside of the wake, not the photon temperature  $T_\gamma$ ). Shock heating is more likely to have occurred for strings laid down earlier. Below we determine the upper cutoff time for shock heating to have occurred.

Note that the later the wake is laid down, the lower the kinetic temperature. This leads to a lower bound on the redshift  $z_m$ , after which the cosmic string wakes will not have undergone shock heating. The kinetic temperature for the gas inside the wake is [2]

$$T_K = [20\text{K}] (G\mu)_6^2 (v_s \gamma_s)^2 \frac{z_m + 1}{z_e + 1}. \quad (17)$$

Until reionization, the background gas is cooling adiabatically below redshifts of  $z \approx 150$  as:

$$T_g = 0.02\text{K} (1 + z_e)^2. \quad (18)$$

The requirement  $T_K > 2.5T_g$  leads to

$$z_m + 1 > \frac{(1 + z_e)^3}{400 (G\mu)_6^2 (v_s \gamma_s)^2}. \quad (19)$$

Only the Hubble steps with  $z_m$  satisfying Eq. (19) lead to wakes where shock heating occurs.

This requirement that only shock heated wakes contribute significantly leads to a maximal number of Hubble steps in the toy model. The Hubble steps that should be taken into account are  $m = 1, \dots, M$ , where

$$M = \text{Int} \left[ \log_2 \left( \frac{t(z_m^{\min}) + t(z_m^{\max})}{t(z_m^{\max})} \right) \right] = \text{Int} \left\{ \log_2 \left[ 1 + \left( \frac{z_m^{\max} + 1}{z_m^{\min} + 1} \right)^{3/2} \right] \right\}, \quad (20)$$

where  $\text{Int}(x)$  denotes the integer part of  $x$ . Later wakes which have not undergone shock heating are thinner (see Eq. 2) and less numerous (see Eq. 12) than the earlier ones. In addition, they are not gravitationally bound due to free streaming. For both of these reasons, their contribution to our power spectrum is negligible.

For example, when we take the 21 cm emission redshift to be  $z_e = 20$ , and set the maximal redshift of cosmic string wake laid down time to be the matter radiation equality time  $z_m^{\max} \simeq 3000$ , then the number of Hubble steps which lead to important cosmic string wake 21 cm emission is as plotted in Fig. 3.

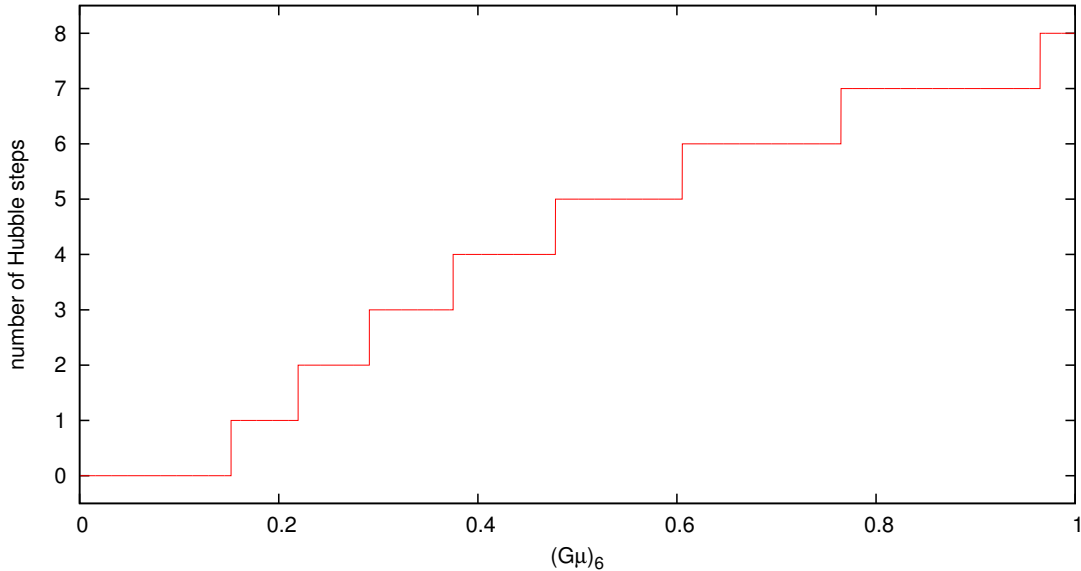


FIG. 3: The number of Hubble steps, for a given string tension, during which a wake emits 21 cm radiation. The parameters used are  $z_e = 20$ ,  $z_m^{\max} = 3000$  and  $v_s^2 \gamma_s^2 = 1/3$ .

#### IV. POWER SPECTRUM

We will compute the angular power spectrum of the 21 cm brightness temperature at a fixed redshift with a string tension larger than the critical value for emission. A few words of warning are in order. Firstly, for a Gaussian distribution the two point function contains all the information about the distribution. However, in the case of cosmic strings, the signal is very non-Gaussian. Hence, the two point correlation function will miss important information. Secondly, one of the advantages of 21 cm surveys compared to other measures (e.g. CMB temperature maps) is that the maps are three dimensional and thus can contain much more information. In restricting attention to a fixed redshift, we are not exploiting this advantage. Nevertheless, in order to compare the 21 cm signal of cosmic strings with that of other sources, it is useful to compute the angular correlation function. We plan to extend our analysis and compute the three dimensional correlation function in upcoming work.

We are performing our calculation in the framework of the toy model distribution of long strings of [12] reviewed earlier. In this analysis, the strings at different Hubble time intervals are statistically independent. Hence, we can first consider a fixed string formation time Hubble interval and sum the results over all redshift intervals which make a contribution. In the following subsection, we therefore consider the contribution from strings in a fixed single Hubble string formation time step.

##### A. A single Hubble step

First we calculate the two point correlation function  $\langle \delta T_b(\mathbf{0}) \delta T_b(\mathbf{x}) \rangle$ . The brackets indicate an ensemble average. We assume the validity of the ergodic hypothesis so that ensemble averages can be computed by volume averages. We shall use the flat sky approximation because we are interested in scales of order ten degrees on the sky or smaller. The position  $\mathbf{x}$  in the two dimensional sky is the 2-d angular coordinate times the radial distance of the fixed redshift surface  $z_e$  under consideration.

Whereas in the three dimensional redshift-angle space a wake is long in two dimensions and narrow in one, the intersection of the wake with the fixed redshift surface produces an object which is long in only one dimension and typically narrow in the second. We will call the size of this second dimension the “projected width”. As illustrated in Fig. 4, the projected width  $\tilde{w}$  of the wake can be written as

$$\tilde{w} = \begin{cases} w/\cos\psi & \text{for } 0 \leq \psi < \pi/2 - \arcsin(w/l) \\ l & \text{for } \pi/2 - \arcsin(w/l) \leq \psi \leq \pi/2 \end{cases}, \quad (21)$$

where  $\psi$  is the angle of the wake relative to the fixed redshift surface.

Since the positions and orientations of different string wakes at a fixed Hubble time step are taken to be random, the computation reduces to the computation of the ensemble average of the contribution of a single string wake. We will consider the ensemble average of the contribution of a single string in a box of dimensions  $L \times L$ , where  $L$  is larger than the length of the wake we are interested in. Since the dominant contribution to the 21 cm signal comes from strings created at about  $t_{\text{eq}}$ , we do not need  $L$  to correspond to a large angular scale. As in the studies of position space signals of cosmic strings to CMB temperature and polarization maps, an angular extent of  $10^\circ$  is more than enough (larger areas will obviously lead to reduced statistical error bars). Returning to the study of the effect of a single string wake, the geometry is illustrated in Fig. 4. Here we assume that the cosmic string wake intersects the surface of fixed redshift  $z_e$ . As discussed in Section III B, the number density of such string wakes is  $n_{2D}$ . We now study the contribution of this string to the correlation function.

When both points  $0$  and  $\mathbf{x}$  are on the wake, the product  $\delta T_b(\mathbf{0})\delta T_b(\mathbf{x})$  contributes  $\overline{\delta T_b^2}$  to the ensemble average. Otherwise, when either points  $0$  or  $\mathbf{x}$  are not on the wake, the product is zero. In this way, the calculation of the ensemble average is reduced to the calculation of probability that both points  $0$  and  $\mathbf{x}$  are on the wake. We have

$$\langle \delta T_b(\mathbf{0})\delta T_b(\mathbf{x}) \rangle = \overline{\delta T_b^2} \times (\text{Probability}) . \quad (22)$$

There are probabilities for both the horizontal and vertical coordinates of the points  $0$  and  $\mathbf{x}$  to be on the wake. When  $0 < \phi < \arctan(l/\tilde{w})$  ( $\phi$  is labeled in Fig. 4), the probability we calculate is a product of these two probabilities:

$$(\text{Probability}) = \begin{cases} \frac{\tilde{w}/\cos\phi - r}{L} \times \frac{l\cos\phi}{L} & \text{for } r < \tilde{w}/\cos\phi \\ 0 & \text{for } r \geq \tilde{w}/\cos\phi \end{cases} , \quad (23)$$

where  $r$  is the magnitude of  $\mathbf{x}$  and  $\tilde{w} \equiv w/\cos\psi$  is the projected width of the wake onto the fixed redshift hypersurface. The angles  $\psi$  and  $\phi$  are shown in Fig. 4. They should be integrated over when performing the ensemble average.

On the other hand, there is the other region  $\arctan(l/\tilde{w}) < \phi < \pi/2$ , which is small on small scales but will give a comparable contribution on large scales (scales of order the length of the wake). In this region, the probability that both points  $0$  and  $\mathbf{x}$  are on the wake can be written as

$$(\text{Probability}) = \begin{cases} \frac{l\sin\phi - r}{L} \times \frac{\tilde{w}/\sin\phi}{L} & \text{for } r < l\sin\phi \\ 0 & \text{for } r \geq l\sin\phi \end{cases} . \quad (24)$$

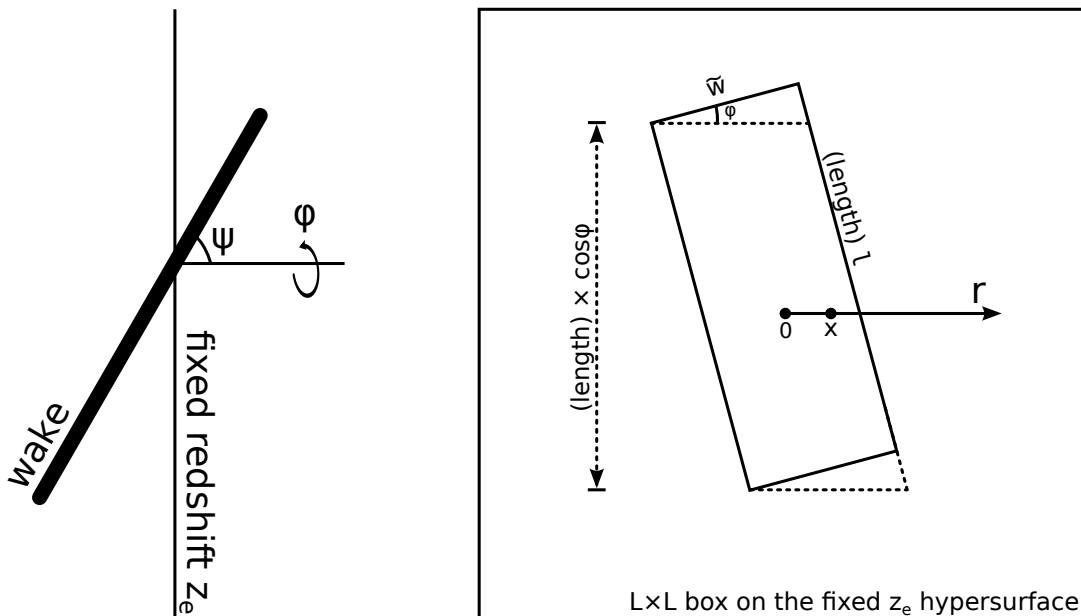


FIG. 4: This figure illustrates the cosmic string wake profile. Both panels represent cross sections through space at the time  $t_e$ . The “fixed redshift hypersurface” is the intersection of our past light cone with this space. The left panel introduces the angles which describe the relative geometry between the wake and the fixed redshift hypersurface, on which the 21 cm signal is emitted. The right panel shows the projection of the wake onto the fixed redshift surface. Here the “width” in the figure is  $\tilde{w}$ , the projected width of the wake.



Based on rotational symmetry of the ensemble, the correlation function will only depend on  $r$ , the magnitude of  $\mathbf{x}$ . For a single wake, the considerations of (22), (23) and (24) yield

$$\begin{aligned} \langle \delta T_b(0) \delta T_b(r) \rangle &= \frac{2\overline{\delta T_b}^2}{\pi L^2} \int_0^{\pi/2} d\psi \int_0^{\arctan(l/\tilde{w})} d\phi \, l \sin \psi (\tilde{w} - r \cos \phi) \Theta(\tilde{w}/\cos \phi - r) \\ &+ \frac{2\overline{\delta T_b}^2}{\pi L^2} \int_0^{\pi/2} d\psi \int_{\arctan(l/\tilde{w})}^{\pi/2} d\phi \, \tilde{w} \sin \psi (l - r/\sin \phi) \Theta(l \sin \phi - r) . \end{aligned} \quad (25)$$

where  $\Theta(x)$  is the Heaviside step function. Note that we have put a normalization factor  $2/\pi$  in front of the integration, because we are averaging over  $1/8$  of the solid angle by restricting  $\psi$  and  $\phi$  to both run from  $0$  to  $\pi/2$ .

The angular power spectrum of zero mean fluctuations is obtained by taking the Fourier transform of the above correlation function and subtracting the square of the brightness temperature times  $(2\pi)^2 \delta_D^2(\vec{k})$  for the zero mode. Hence for  $k \neq 0$  the contribution of a single string wake can be written as

$$P_1(k) = \int_0^\infty dr \int_0^{2\pi} d\theta \, r e^{-ikr \cos \theta} \langle \delta T_b(0) \delta T_b(r) \rangle , \quad (26)$$

where  $r, \theta$  are the polar coordinates of  $\mathbf{x}$ . One can insert Eq. (25) into Eq. (26), integrate out  $\theta, r, \phi$  and  $\psi$  to obtain the power spectrum on length scales much smaller than the wake length  $l$ . In this regime, the power spectrum can be well approximated by

$$P_1(k) = \frac{4l\overline{\delta T_b}^2}{L^2 k^3} [1 - \cos(wk) - wk \text{Si}(wk) + wk \text{Si}(lk)] , \quad (27)$$

where  $\text{Si}(z)$  is the sin integral defined as  $\text{Si}(z) \equiv \int_0^z dt (\sin t)/t$ . On the other hand, on scales larger than the wake length  $l$ , the power spectrum  $P_1(k)$  is independent on  $k$ . This can be seen by taking the limit  $k \rightarrow 0$  in Equation (26). The full power spectrum can be calculated numerically.

Now we will consider multiple cosmic string wakes which are laid down within the same Hubble time step. Up to a factor of order one, these cosmic string wakes have the same dimensions as calculated in Section III B. If we assume these wakes do not have any cross correlations between each other, then we simply have to multiply the result for a single string wake by the number of string wakes in the observation area, which is  $L^2 n_{2D}$ . Thus, the result for multiple string wakes (single Hubble time step) in the region  $kl \gg 1$  becomes

$$P(k) = \frac{4ln_{2D}\overline{\delta T_b}^2}{k^3} [1 - \cos(wk) - wk \text{Si}(wk) + wk \text{Si}(lk)] . \quad (28)$$

On scales much smaller than the wake length  $l$ , the dimensionless power spectrum <sup>2</sup> can be written as

$$\Delta(k) \equiv \frac{k^2}{2\pi} P(k) = \frac{2ln_{2D}\overline{\delta T_b}^2}{\pi k} [1 - \cos(wk) - wk \text{Si}(wk) + wk \text{Si}(lk)] . \quad (29)$$

Eq. (29) and the corresponding numerical result (shown in Fig. 5) are the main result of our paper.

Since, as mentioned earlier,  $P(k)$  is constant in the limit of small values of  $k$ ,  $\Delta(k)$  scales  $k^2$  for small  $k$ . The scaling for large values of  $k$  is  $k^{-1}$ , which can be obtained by expanding Eq. (29) in a power series.

It is also convenient to use  $wk$  as the argument and rewrite the dimensionless power spectrum (for  $kl > 1$ ) as

$$\frac{\Delta(k)}{wn_{2D}\overline{\delta T_b}^2} = \frac{2}{\pi wk} \left[ 1 - \cos(wk) - wk \text{Si}(wk) + wk \text{Si}\left(\frac{l}{w} \times wk\right) \right] . \quad (30)$$

Eq. (30) is plotted in Fig. 5. Note that the dimensionless power spectrum is almost scale invariant between the scales  $1/l < k < 1/w$  corresponding to the wake length and the wake width. When  $k < 1/l$  it decays as  $k^2$ , and when  $k > 1/w$  it decreases as  $k^{-1}$ .

<sup>2</sup> Here dimensionless means that there is no  $k$  dimension. The power spectrum still has dimension of temperature squared.

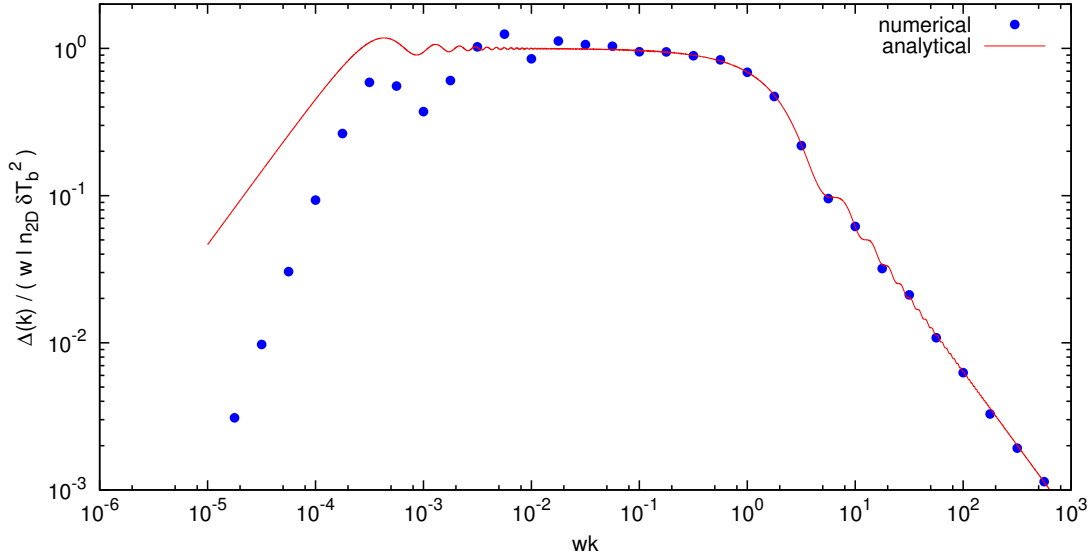


FIG. 5: The dimensionless power spectrum  $\Delta(k)$ . We plot  $\Delta(k)/(wn_{2D}\overline{\delta T_b^2})$  as a function of  $wk$ . In the plot we take  $l/w$  to be 9000. This value is calculated using  $z_e = 20$ ,  $z_m = 3000$ ,  $(G\mu)_6 = 0.2$ ,  $v_s = 1/2$ , and  $\cos^2\theta_s = 1/2$ .

As an example, we consider  $(G\mu)_6 = 0.2$  (around the current upper bound on the string tension),  $z_e = 20$  and  $N_H = 10$  strings per Hubble volume. From Fig. 3 we see that only wakes from a single Hubble time step undergo shock heating. The relevant length scales of the wakes are

$$w = 2.3 \times 10^{-4} \text{Mpc} , \quad l = 2.1 \text{Mpc} . \quad (31)$$

The number density of wakes from Eq. 12, and the induced 21 cm brightness temperature from Eq. 3 are

$$n_{2D} = 0.12 \text{Mpc}^{-2} , \quad \overline{\delta T_b} = -15 \text{mK} . \quad (32)$$

In this case, the dimensionless power spectrum becomes

$$\Delta(k) \simeq 8000 \mu\text{K}^2 \quad \text{for } 1/l < k < 1/w . \quad (33)$$

Comparing this result with the square of the local brightness temperature from (3) we see that the power spectrum is suppressed by a significant factor. This is a reflection of the highly non-Gaussian distribution of wakes in space, and the resulting highly non-Gaussian distribution of the string-induced wedges in the 21cm brightness maps. The fraction of the 21cm sky at a fixed redshift which is covered by string-induced wedges is proportional to  $w/l \sim G\mu$ . Thus, whereas the local brightness temperature inside a 21cm wedge is to a first approximation independent of the cosmic string tension, the two-dimensional power spectrum decreases in amplitude as  $G\mu$  decreases. The dependence on  $G\mu$  is linear as can be seen from (30), since in the flat portion of the spectrum the last term in the square brackets dominates.

Finally we also would like to comment which features of the power spectrum are expected to exist for a realistic cosmic string network and which features are artifacts of the toy model.

The decay rates of  $\Delta(k)$  at small and large values of  $k$  should be robust because they do not depend on special assumptions made in the cosmic string toy model. We also trust the nearly scale invariant behavior between  $1/l$  and  $1/w$ .

However, the oscillations seen in the spectrum near  $k = 1/l$  are probably an artifact of the toy model. This is because we have assumed all string wakes are laid down at one particular redshift  $z_m$ . This is not accurate (up to an order one factor) even in the case that only one Hubble step is needed. String wakes laid down at different  $z_m$  are expected to lead to cancellations because of the different phases of oscillation. We also expect that the spectrum should have a slight blue tilt near  $k = 1/l$ . This is because the larger scale wakes are laid down at later times and thus lead to a lower brightness temperature.

## B. Multiple Hubble steps

We now consider the case when there are several Hubble steps which lead to wakes with  $T_K < 2.5T_g$ . In this situation, the power spectrum becomes a superposition of the power spectra in different Hubble steps. For example,

when we are considering measurements for emission redshift  $z_e = 20$ , then when  $(G\mu)_6 > 0.22$ , multiple Hubble steps are necessary.

We assume no cross correlation between string wakes in different Hubble steps. Then, the contribution from different Hubble steps can be added together directly. In the left and right panels of Fig. 6, we plot the dimensionless power spectrum from wakes at each Hubble step and the sum, respectively. Note that the first Hubble step has the largest brightness temperature. Thus the first step dominates the total power spectrum.

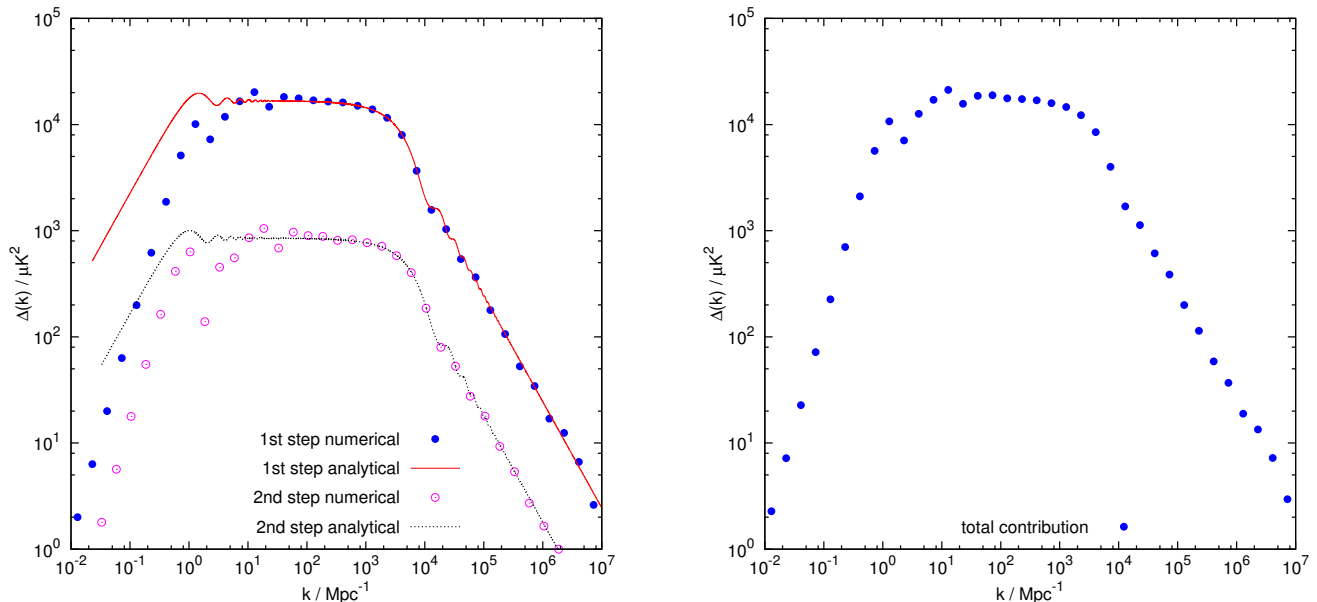


FIG. 6: The dimensionless power spectrum from string wakes at individual Hubble steps (left), and the sum over the steps (right). The parameters are  $z_e = 20$ ,  $z_m^{\text{max}} = 3000$ ,  $(G\mu)_6 = 0.3$ ,  $v_s = 1/2$ ,  $\cos^2 \theta_s = 1/2$ , and  $N_H = 10$ .

## V. CONCLUSION

We have computed the angular power spectrum of 21 cm emission (at a fixed redshift) from a scaling distribution of string wakes. Wakes from strings present near the time of equal matter and radiation, dominate the spectrum. The dimensionless power spectrum scales as  $k^2$  on long distance scales and as  $k^{-1}$  on short distances. In the above, “long” is relative to the length of the string wake which corresponds to an angular scale of about  $0.1^\circ$  and which is independent of the string tension. “Short” is relative to the width of the wake which depends on the string tension (its order of magnitude is  $G\mu$  times the length of the wake. On intermediate scales, the spectrum is roughly scale-invariant.

The above features of the 21 cm power spectrum from string wakes are robust against details of the string wake scaling solution. The overall amplitude, however, depends quite sensitively on the details. As an example, let us consider the redshift  $z_e = 20$ , larger than the redshift of reionization so that we do not need to worry about “noise” from reionization processes. Then, for  $(G\mu)_6 = 0.2$  (the current upper bound on the string tension, and assuming 10 string segments per Hubble volume, the amplitude of the dimensionless power spectrum over the flat part of the spectrum is of the order  $\Delta(k)^{1/2} \simeq 90 \mu\text{K}$ . This amplitude is significantly smaller than the local brightness temperature in a string-induced 21cm wedge in position space. Whereas the local brightness temperature in position space is to a first approximation independent of the string tension, the two-dimensional power spectrum decreases linearly with  $G\mu$  as the string tension decreases. This difference between the local and the root mean square power of the signal is a reflection of the highly non-Gaussian distribution of cosmic string wakes, and it reinforces the lesson learned from studies of cosmic string imprints on CMB temperature maps - namely that it is easier to detect the signatures of cosmic strings when analyzing the data in position space.

It will be of great interest to study in detail the detectability of this signal with upcoming and planned experiments. To put the predicted amplitude into some context, let us recall that the current strongest upper bound on a cosmological 21 cm signal is 70 mK [25] on angular scales of about  $3.3^\circ$ . The redshift range probed in this experiment (GMRT) lies between 8.1 and 9.2. One foreground for our signal is the power spectrum induced by mini-halos, nonlinearities which result from the Gaussian primordial fluctuations. An analytical estimate of the effect was given in [26], with

the predicted spectrum  $\Delta(k)^{1/2}$  at redshift  $z = 15$  peaking at  $k \simeq 10^3 h\text{Mpc}^{-1}$  at an amplitude of about 100 mK and decaying linearly with  $k$  for smaller values of  $k$ . A detailed numerical study of the expected signal of reionization effects at a redshift of  $z = 11$  was performed in [27] yielding a spectrum which peaks at 10mK at a value of the angular quantum number  $l$  of  $l \sim 10^4$  and decaying roughly linearly with  $l$  for smaller values of  $l$ , and turning flat for larger values. Turning to low redshift surveys, we recall that 21 cm experiments are planned to be able to pick out a  $20\mu\text{K}$  signal from baryon acoustic oscillations from a noise of 300mK from large-scale structure on a length scale of about 8Mpc [28]. Thus, it appears to us that the predicted spectrum from a scaling distribution of cosmic string wakes is large and has a good chance of being visible in the planned high redshift surveys.

Our work is based on a simple toy model for the distribution of cosmic strings which captures the main properties of string networks. Cosmic string loops and wiggles on long strings are, however, not contained in the present toy model. It would be of interest to extend our work to capture these aspects of real string networks.

The restriction to fixed emission redshift cuts down a lot of the information which is contained in 21 cm redshift maps. Hence, it will be of great interest to extend our analysis and calculate the three dimensional redshift power spectrum of 21 cm emission from cosmic strings. Work on this topic is ongoing.

### Acknowledgment

This research is supported in part by an NSERC Discovery Grant, by funds from the CRC program, and by a Killam Research Fellowship to R.B.. Y.W. acknowledges support from grants from McGill University, Fonds Quebecois de la Recherche sur la Nature et les Technologies (FQRNT), the Institute of Particle Physics (Canada) and the Foundational Questions Institute. O.H. is supported in part by the FQRNT Programme de recherche pour les enseignants de collège. We are grateful for useful discussions with Rebecca Danos, Matt Dobbs, Gil Holder and Ue-li Pen. We thank Rebecca Danos for producing Figure 1 for us.

- 
- [1] S. Furlanetto, S. P. Oh and F. Briggs, “Cosmology at Low Frequencies: The 21 cm Transition and the High-Redshift Universe,” *Phys. Rept.* **433**, 181 (2006) [arXiv:astro-ph/0608032].
  - [2] R. H. Brandenberger, R. J. Danos, O. F. Hernandez and G. P. Holder, “The 21 cm Signature of Cosmic String Wakes,” *JCAP* **1012**, 028 (2010) [arXiv:1006.2514 [astro-ph.CO]].
  - [3] A. Vilenkin and E.P.S. Shellard, *Cosmic Strings and other Topological Defects* (Cambridge Univ. Press, Cambridge, 1994).
  - [4] M. B. Hindmarsh and T. W. B. Kibble, “Cosmic strings,” *Rept. Prog. Phys.* **58**, 477 (1995) [arXiv:hep-ph/9411342].
  - [5] R. H. Brandenberger, “Topological defects and structure formation,” *Int. J. Mod. Phys. A* **9**, 2117 (1994) [arXiv:astro-ph/9310041].
  - [6] J. H. P. Wu, P. P. Avelino, E. P. S. Shellard, B. Allen, “Cosmic strings, loops, and linear growth of matter perturbations,” *Int. J. Mod. Phys. D* **11**, 61-102 (2002). [astro-ph/9812156].
  - [7] R. Durrer, M. Kunz, A. Melchiorri, “Cosmic structure formation with topological defects,” *Phys. Rept.* **364**, 1-81 (2002). [astro-ph/0110348].
  - [8] R. Jeannerot, “A Supersymmetric SO(10) Model with Inflation and Cosmic Strings,” *Phys. Rev. D* **53**, 5426 (1996) [arXiv:hep-ph/9509365];  
R. Jeannerot, J. Rocher and M. Sakellariadou, “How generic is cosmic string formation in SUSY GUTs,” *Phys. Rev. D* **68**, 103514 (2003) [arXiv:hep-ph/0308134].
  - [9] S. Sarangi and S. H. H. Tye, “Cosmic string production towards the end of brane inflation,” *Phys. Lett. B* **536**, 185 (2002) [arXiv:hep-th/0204074].
  - [10] T. W. B. Kibble, “Phase Transitions In The Early Universe,” *Acta Phys. Polon. B* **13**, 723 (1982);  
T. W. B. Kibble, “Some Implications Of A Cosmological Phase Transition,” *Phys. Rept.* **67**, 183 (1980).
  - [11] A. Albrecht and N. Turok, “Evolution Of Cosmic Strings,” *Phys. Rev. Lett.* **54**, 1868 (1985);  
D. P. Bennett and F. R. Bouchet, “Evidence For A Scaling Solution In Cosmic String Evolution,” *Phys. Rev. Lett.* **60**, 257 (1988);  
B. Allen and E. P. S. Shellard, “Cosmic String Evolution: A Numerical Simulation,” *Phys. Rev. Lett.* **64**, 119 (1990);  
C. Ringeval, M. Sakellariadou and F. Bouchet, “Cosmological evolution of cosmic string loops,” *JCAP* **0702**, 023 (2007) [arXiv:astro-ph/0511646];  
V. Vanchurin, K. D. Olum and A. Vilenkin, “Scaling of cosmic string loops,” *Phys. Rev. D* **74**, 063527 (2006) [arXiv:gr-qc/0511159].
  - [12] L. Perivolaropoulos, “COBE versus cosmic strings: An Analytical model,” *Phys. Lett. B* **298**, 305 (1993) [arXiv:hep-ph/9208247].
  - [13] Y. B. Zeldovich, “Cosmological fluctuations produced near a singularity,” *Mon. Not. Roy. Astron. Soc.* **192**, 663 (1980);  
A. Vilenkin, “Cosmological Density Fluctuations Produced By Vacuum Strings,” *Phys. Rev. Lett.* **46**, 1169 (1981) [Erratum-ibid. **46**, 1496 (1981)].

- [14] A. Vilenkin, “Gravitational Field Of Vacuum Domain Walls And Strings,” *Phys. Rev. D* **23**, 852 (1981).
- [15] N. Kaiser and A. Stebbins, “Microwave Anisotropy Due To Cosmic Strings,” *Nature* **310**, 391 (1984).
- [16] S. Amsel, J. Berger and R. H. Brandenberger, “Detecting Cosmic Strings in the CMB with the Canny Algorithm,” *JCAP* **0804**, 015 (2008) [arXiv:0709.0982 [astro-ph]];  
A. Stewart and R. Brandenberger, “Edge Detection, Cosmic Strings and the South Pole Telescope,” *JCAP* **0902**, 009 (2009) [arXiv:0809.0865 [astro-ph]];  
R. J. Danos and R. H. Brandenberger, “Canny Algorithm, Cosmic Strings and the Cosmic Microwave Background,” *Int. J. Mod. Phys. D* **19**, 183 (2010) [arXiv:0811.2004 [astro-ph]];  
R. J. Danos and R. H. Brandenberger, “Searching for Signatures of Cosmic Superstrings in the CMB,” *JCAP* **1002**, 033 (2010) [arXiv:0910.5722 [astro-ph.CO]].
- [17] J. Canny, “A computational approach to edge detection”, *IEEE Trans. Pattern Analysis and Machine Intelligence* **8**, 679 (1986).
- [18] J. E. Ruhl *et al.* [The SPT Collaboration], “The South Pole Telescope,” *Proc. SPIE Int. Soc. Opt. Eng.* **5498**, 11 (2004) [arXiv:astro-ph/0411122].
- [19] A. Kosowsky [the ACT Collaboration], “The Atacama Cosmology Telescope Project: A Progress Report,” *New Astron. Rev.* **50**, 969 (2006) [arXiv:astro-ph/0608549].
- [20] J. Silk and A. Vilenkin, “Cosmic Strings And Galaxy Formation,” *Phys. Rev. Lett.* **53**, 1700 (1984);  
M. Rees, “Baryon concentrations in string wakes at  $z \geq 200$ : implications for galaxy formation and large-scale structure,” *Mon. Not. R. astr. Soc.* **222**, 27p (1986);  
T. Vachaspati, “Cosmic Strings and the Large-Scale Structure of the Universe,” *Phys. Rev. Lett.* **57**, 1655 (1986).
- [21] A. Stebbins, S. Veeraraghavan, R. H. Brandenberger, J. Silk and N. Turok, “Cosmic String Wakes,” *Astrophys. J.* **322**, 1 (1987);  
R. H. Brandenberger, L. Perivolaropoulos and A. Stebbins, “Cosmic Strings, Hot Dark Matter and the Large-Scale Structure of the Universe,” *Int. J. Mod. Phys. A* **5**, 1633 (1990).
- [22] Y. B. Zeldovich, “Gravitational instability: An Approximate theory for large density perturbations,” *Astron. Astrophys.* **5**, 84 (1970).
- [23] B. Zygelman, Hyper-fine Level-changing Collisions of Hydrogen Atoms and Tomography of the Dark Age Universe, *Astrophys. J.* **622**, 1356 (2005);  
S. Furlanetto and M. Furlanetto, “Spin Exchange Rates in Electron-Hydrogen Collisions,” *Mon. Not. Roy. Astron. Soc.* **374**, 547 (2007) [arXiv:astro-ph/0608067].
- [24] M. Kuhlen, P. Madau and R. Montgomery, “The spin temperature and 21cm brightness of the intergalactic medium in the pre-reionization era,” *Astrophys. J.* **637**, L1 (2006) [arXiv:astro-ph/0510814].
- [25] G. Paciga, T. -C. Chang, Y. Gupta, R. Nityanada, J. Odegova, U. -L. Pen, J. Peterson, J. Roy *et al.*, “The GMRT-EoR Experiment: A new upper limit on the neutral hydrogen power spectrum at  $z$  8.6,” [arXiv:1006.1351 [astro-ph.CO]].
- [26] J. Kim, U. -L. Pen, “Redshifted 21-cm Signals in the Dark Ages,” [arXiv:0908.1973 [astro-ph.CO]].
- [27] P. R. Shapiro, I. T. Iliev, G. Mellema, U. -L. Pen, H. Merz, “The Theory and Simulation of the 21-cm Background from the Epoch of Reionization,” *AIP Conf. Proc.* **1035**, 68-74 (2008). [arXiv:0806.3091 [astro-ph]].
- [28] J. B. Peterson, R. Aleksan, R. Ansari, K. Bandura, D. Bond, J. Bunton, K. Carlson, T. -C. Chang *et al.*, “21 cm Intensity Mapping,” [arXiv:0902.3091 [astro-ph.IM]].